

A frequency-tuned magnetic resonance-based wireless power transfer system with near-constant efficiency up to 24 cm distance

Seyit Ahmet SİS^{1,*} , Selçuk KAVUT² 

¹Department of Electrical & Electronics Engineering, Faculty of Engineering, Balıkesir University, Balıkesir, Turkey

²Department of Computer Engineering, Faculty of Engineering, Balıkesir University, Balıkesir, Turkey

Received: 14.03.2018

Accepted/Published Online: 23.07.2018

Final Version: 29.11.2018

Abstract: In magnetic resonance-based wireless power transfer systems, the main challenge arises from varying distances between coils during power transfer because distance variations ultimately reduce the power transfer efficiency. Frequency-tuned wireless power transfer systems provide an almost-constant output power to the load up to a critical coupling distance. However, the critical coupling distance and power transfer efficiency are dependent on coil size, source, and load resistances. The purpose of this paper is to discuss this dependency with an equivalent circuit model, determine a suitable coil size for given design specifications, and set up a frequency-tuned system that is based on tracking the resonance frequency at the transmitter side. The coil's lateral size is usually limited by the size of the device to be charged in wireless power transfer applications; therefore, radii of coils are fixed to 25 cm. Coil size is varied by changing the number of turns during simulations. Two identical coils are fabricated based on the simulations using an equivalent circuit model and characterized by S-parameter measurements. A frequency-tuned system is then realized using the fabricated coils, a radiofrequency bidirectional coupler, and a suitable load resistance. Measured power transfer efficiency exhibits good agreement with that predicted by the circuit model. An almost-constant power transfer efficiency of more than 75 % is obtained for up to 24 cm coil separations.

Key words: Frequency-tuned, wireless power transfer, wireless charging, frequency splitting, coil design

1. Introduction

Coupling between coils in magnetic resonance-based wireless power transfer systems is quite sensitive to separation and misalignment between the coils. Therefore, usually the system is optimized for a fixed transfer distance and good alignment between the coils [1–3]. However, recent developments in magnetic resonance-based wireless power transfer systems pave the way for coupling-independent power transfer to some extent [4–21]. For example, impedance-tuned systems utilize adaptive matching systems at transmit and receive coils [4–7]. Some tunable radiofrequency components and a controller unit are needed in such systems. Other approaches to increase the tolerance of wireless power systems to distance and misalignment variations include utilization of multiple-component compensation topologies and polarized coils [9–11]. The series-parallel-series (SPS) compensation topology in [11] exhibits up to 25 % improvement in tolerance to the misalignment. Polarized coils such as flux-pipe and double-D (DD) structures exhibit significant improvements in misalignment tolerance of coupling coefficients [9, 10]. Frequency tuning mechanisms are also proposed for realizing distance-variation and misalignment-tolerant systems [12–21]. Frequency-tuned systems utilize the frequency splitting behavior of

*Correspondence: seyit.sis@balikesir.edu.tr

coupled resonant coils operating in a strongly coupled regime. Almost-constant peak power transfer efficiency (η_{\max}) can be obtained at two split resonance frequencies called f_{odd} and f_{even} , as the distance between the coils varies as long as the distance is less than the critical coupling distance (d_{critical}) [22, 23]. f_{odd} and f_{even} are slightly lower and higher frequencies than the resonance frequency (f_0) of uncoupled resonant coils, respectively, and vary as the coupling between coils changes. Therefore, the source frequency is tuned to either one of these frequencies for ensuring peak power efficiency as the distance varies. A major drawback in frequency-tuned systems would be the frequency band limitations of government regulations; however, frequency-tuned systems may still find applications inside shielded areas or at low frequencies, which are not suitable for wireless communication (e.g., electrical vehicle (EV) chargers). In frequency-tuned systems, there is a trade-off between η_{\max} and d_{critical} , which are predominantly influenced by the coil size (i.e. number of turns for each coil), source, and load resistances (R_S and R_L). Imura et al. [22, 23] very well explained the effect of R_S and R_L on power transfer efficiency through experiments. They showed that larger R_S and R_L values result in larger peak efficiency values at the cost of reduced critical coupling distances. Similar observations can be made using circuit model-based simulations for unequal R_S and R_L values, as well.

1.1. Contributions

In this paper, we present a frequency-tuned wireless power transfer system that exhibit a near-constant efficiency of more than 75 % for up to 24 cm coil separation. An equivalent circuit model is utilized for choosing suitable coil size (number of turns), source, and load resistances for the given design specifications in terms of peak efficiency and distance. While utilizing the circuit model, possible solutions for source and load resistances (R_S and R_L) satisfying the given design specs are plotted in 2-Dimensional (2D) graphs for various numbers of turns for the coils. Therefore, a detailed analysis of the effect of R_S , R_L , and number of turns on power transfer efficiency and critical coupling distance is provided. A pair of identical coils is fabricated and characterized using a vector network analyzer. The coils are then utilized in the aforementioned frequency-tuned system, which employs an radio frequency (RF) signal generator, an RF bidirectional coupler and a suitable load resistance. To the best of the authors' knowledge, this paper presents the first systematical way for choosing the optimal number of turns to reach given design specifications in terms of efficiency and the distance for frequency-tuned wireless power transfer systems.

2. Equivalent circuit model and efficiency expression

An equivalent circuit model (lumped element model) for magnetic resonance-based wireless power transfer systems is shown in Figure 1. Series-connected external capacitors are utilized to resonate the coils. The mutual inductance (M) represents the level of magnetic coupling between the coils and is dependent also on the distance between the coils. Assuming the transmit and receive coils are identical, self-inductance of each coil can be calculated as follows [24]:

$$L_1 = L_2 = N^2 \mu_0 \sqrt{(r-a)(r+a)} \left[\left(\frac{2}{k} - k \right) K(k) - \left(\frac{2}{k} \right) E(k) \right], \quad (1)$$

where K and E are the complete elliptic integrals of the first and second kind, as follows:

$$K(k) = \int_0^{\frac{\pi}{2}} \frac{d\beta}{\sqrt{1 - k^2 \sin^2 \beta}}, \quad (2)$$

$$E(k) = \int_0^{\frac{\pi}{2}} d\beta \sqrt{1 - k^2 \sin^2 \beta}, \quad (3)$$

$$k = \sqrt{\frac{4(r - a)(r + a)}{(2r)^2 + (2a)^2}}. \quad (4)$$

μ_0 , N , a , and r are the magnetic permeability of the air, number of turns, radius of the wire, and radius of the coil, respectively. The values of series-connected capacitors C_1 and C_2 in Figure 1 are chosen to provide a series LC resonance at the design frequency.

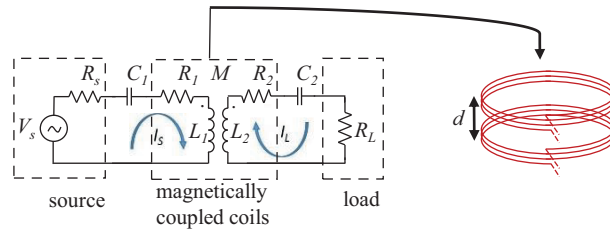


Figure 1. Circuit model for the magnetic resonance-based wireless power transfer system.

The $R_{1,2}$ in the model represents the total radiation, R_r , and conductor, R_c , losses for each coil and can be calculated as follows:

$$R_c = \frac{2\pi r N}{2\pi a} \sqrt{\frac{\mu_0 \omega}{2\sigma}}, \quad (5)$$

$$R_r = 20N^2\pi^2 \left(\frac{2\pi r}{\lambda}\right)^4, \quad (6)$$

$$R_{1,2} = R_c + R_r, \quad (7)$$

where ω is the radial frequency, λ is the wavelength at the operating frequency, and σ is the conductivity of the wire. The mutual inductance, M , between the coils can be calculated as a function of coil geometry and separation between the coils, d , as follows:

$$M = \mu_0 \sqrt{r_1 r_2} \left(\left(\frac{2}{l} - l \right) K(l) - \frac{2}{l} E(l) \right), \quad (8)$$

where K and E are complete elliptic integrals of the first and second kind as in Eqs. (2) and (3), and

$$l = \sqrt{\frac{4r_1 r_2}{(r_1 + r_2)^2 + d^2}}. \quad (9)$$

In Eq. (9), r_1 and r_2 are the radius of each coil. Using the circuit model given in Figure 1, one can calculate

power transfer efficiency, η , as the ratio of the power transferred to the load, P_L , to the power available from the source, P_{AVS} , as given in Eq. (10):

$$\eta = \frac{4R_S R_L \omega^2 M^2}{x_1^2 + x_2^2}, \tag{10}$$

where

$$x_1 = \left[(R_1 + R_S) \left(\omega L_2 - \frac{1}{\omega C_2} \right) + (R_2 + R_L) \left(\omega L_1 - \frac{1}{\omega C_1} \right) \right], \tag{11}$$

$$x_2 = \left[(R_1 + R_S)(R_2 + R_L) - \left(\omega L_1 - \frac{1}{\omega C_1} \right) \left(\omega L_2 - \frac{1}{\omega C_2} \right) + \omega^2 M^2 \right]. \tag{12}$$

3. Power transfer efficiency and critical coupling distance

Coupled loops can operate in a strongly coupled regime or a weakly coupled regime depending on the mutual inductance M between the loops, losses of each loop, and source and load resistances (R_S and R_L). To better explain coupling regimes and existing resonance frequencies in these regimes, a typical power transfer efficiency (η) as a function of frequency for two coupled identical resonant loops, for various M values, is shown in Figure 2a. Each loop is resonant at ω_0 for achieving a maximum efficiency value. As seen in Figure 2a, when M values are lower than M_3 (e.g., M_1, M_2), peak efficiency is observed at ω_0 and increases with increasing M . This is the typical efficiency characteristic of coupled resonant loops operating in a weakly coupled regime. In this regime, since peak efficiency is strongly dependent on M , one needs to vary the input power level accordingly to compensate efficiency variations when the distance and alignment change during power transfer.

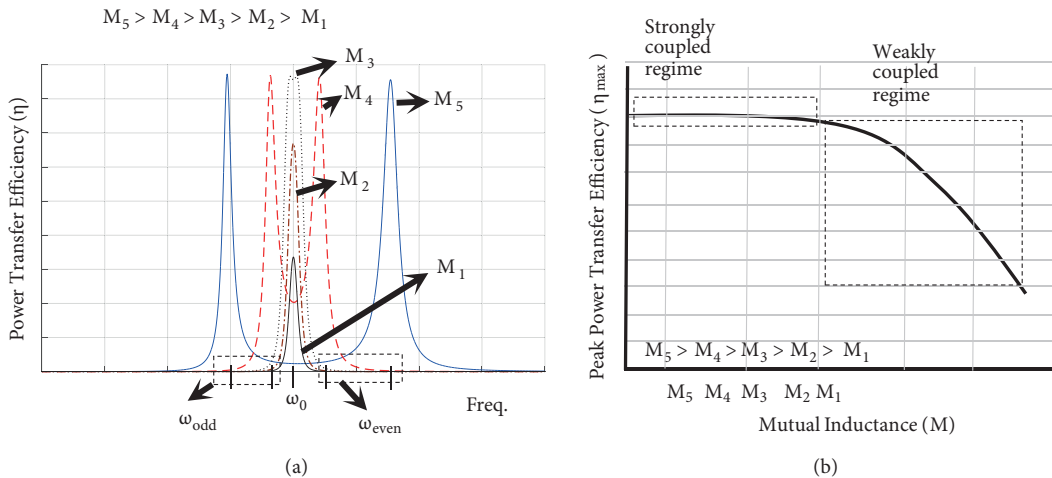


Figure 2. (a) A typical power transfer efficiency response for magnetically coupled resonant loops for various mutual inductance values, M . As M increases, efficiency peaks split from a single resonance frequency of ω_0 to two resonance frequencies of ω_{odd} and ω_{even} . (b) The peak efficiency values for each efficiency response as a function of mutual inductance.

If the coupling level is increased (e.g., by bringing the coils closer) and the M value increases to M_3 , efficiency reaches its maximum value. This value of M , M_3 , is called the critical coupling level. Beyond the

critical coupling level where M values are larger than M_3 (e.g., M_4 , M_5), the resonance peak at ω_0 splits into two efficiency peaks, which separate as M increases (Figure 2a). These two emerging resonance frequencies are called ω_{odd} and ω_{even} , which are at lower and higher frequencies of ω_0 , respectively, as shown in Figure 2a. The key point here is that the peak efficiency values are independent of M in the strongly coupled regime. Therefore, one can deliver a constant power to the load even if the distance and alignment between transmit and receive coils vary during power transfer in a strongly coupled regime. However, to achieve that, the RF source frequency at the transmitter side needs to be tuned to either one of ω_{odd} or ω_{even} because ω_{odd} and ω_{even} vary with mutual inductance in a strongly coupled regime (Figure 2a). Figure 2b shows the peak efficiency values, η_{max} , as a function of mutual inductance and indicates the areas for strongly and weakly coupled regimes in dashed boxes. It should be noted that M values are in descending order on the x-axis of Figure 2b. In this work, we aimed to establish a frequency-tuned wireless power transfer system that exhibits a near-constant efficiency up to a minimum 20 cm distance between coils. Furthermore, we wanted to have more than 90 % efficiency in this distance range. To achieve these specs, the size of coils (e.g., number of turns), source resistance (R_S), and load resistance (R_L) should be chosen carefully for the desired efficiency level and transfer distance range over which a constant efficiency is aimed. There is a trade-off between peak efficiency and critical coupling distance in the strongly coupled regime, and this trade-off can be engineered by the aforementioned parameters (R_S , R_L , and coil size) [22, 23]. Using Eq. (10), η can be simulated as a function of frequency as in Figure 2a. From these simulations, one can computationally determine the maximum efficiency η_{max} for various design parameters, (i.e. separation between the coils, R_S & R_L , number of turns N for each coil, and their radii (r_1 & r_2)). Keeping in mind that the peak efficiency η_{max} stays almost-constant until the critical coupling distance and degrades beyond it, Algorithm 1 can be utilized to extract the approximate values of η_{max} and d_{critical} for fixed values of the aforementioned parameters μ_0 , a , and σ . Using Algorithm 1, solutions of R_L and R_S satisfying the given design specifications (e.g., $\eta_{\text{max}} > 0.9$ and $d_{\text{critical}} > 20$ cm) can be extracted for various coil sizes. Such solutions can be utilized as a design guide when choosing a suitable coil size and source and load resistances. We have performed Algorithm 1 by changing both R_S and R_L from 1 to 100 for number of turns, Ns , of 3, 5, 7, and 9, respectively. Considering the typical sizes of devices to be charged in practical applications, increasing the coil size through its radius seems not very practical. Therefore, we fixed the radius to be 25 cm and changed the size of coils only through the number of turns. The coils are resonated out at 1 MHz ($\omega_0/2\pi$) with series-connected capacitors. In Figure 3, a set of graphs show solutions of R_S and R_L for peak efficiencies larger than 0.9 (90 %) and critical coupling distances larger than 20 cm for various coil sizes (number of turns). The plots in Figure 3 are given for number of turns from three to nine at only odd numbers to cover as large turns as possible; however, one can include the even number of turns as well. Any point on the graphs in Figure 3 represents a peak efficiency and a critical coupling distance value; therefore, corresponding values on the x- and y-axes are the solutions of R_S and R_L for that point, respectively. To better show peak efficiency and critical coupling distance values on the graphs, their values are given in different spans with different colors.

As seen in Figures 3a–3d, as the size of coils (number of turns, Ns) increases from three to five, then to seven and finally nine, more solutions of R_S and R_L arise and the solutions move toward larger values of R_S and R_L . This is because mutual inductance increases for larger coils and hence results in more R_S and R_L solutions for the given design specifications. However, electrical loss resistances also increase with coil size, making them comparable with R_S and R_L values; therefore, small values of R_S and R_L cannot satisfy the given efficiency specifications. For example, when the number of turns is three, available R_S and R_L solutions are mainly limited to below 15 Ω as seen in Figure 3a. On the other hand, coils with nine turns do not have R_S

Algorithm 1: Computation of critical distance (d_{critical}) and efficiency (η_{max}).

Input : Resonance frequency (ω_0), coil size (r_1 , r_2 , and N), source and load resistances (R_S & R_L)

Output: Critical distance (d_{critical}) and efficiency (η_{max}) at strongly coupled regime

```

1  $\eta_{\text{max}} \leftarrow$  Efficiency at  $\omega_0$  for  $d = 1$ ,  $R_S$ ,  $R_L$ ,  $r_1$ ,  $r_2$  and  $N$ ;
2 while (1);
3 {
4      $d \leftarrow d + 1$ ;
5      $\eta \leftarrow$  Efficiency at  $\omega_0$  for  $d$ ,  $R_S$ ,  $R_L$ ,  $r_1$ ,  $r_2$  and  $N$ ;
6     if ( $\eta_{\text{max}} > \eta$ );
7     {
8          $d_{\text{critical}} \leftarrow d - 1$ ;
9         break;
10    }
11     $\eta_{\text{max}} \leftarrow \eta$ ;
12 }
```

and R_L solutions less than approximately 15Ω (Figure 3d). A final conclusion from Figure 3 is the observation of the trade-off between critical coupling distance and peak power transfer efficiency, η_{max} . For all coil sizes (number of turns), it is clear that solutions of R_S and R_L for larger efficiency values result in smaller critical coupling distances.

In other words, the larger the peak efficiency, the smaller the distance over which this efficiency can be constantly achieved. This has been very well explained in Imura and Hori's work through measurement results [22]. Here the graphs in Figure 3 provide a different visualization for this trade-off. It should be noted that parasitic interwinding capacitance and proximity losses, which are limiting factors for increasing the number of turns in multiturn coils, have not been considered in the model.

One can use plots similar to the ones in Figure 3 as a tool for choosing suitable coil size and R_S and R_L values. In this work, we utilize an RF signal generator with 50Ω impedance; therefore, to avoid using an input matching circuit in the frequency-tuned system, R_S is fixed to 50Ω . No solution of $R_S = 50 \Omega$ exists to satisfy design specifications for coils with three turns as shown in Figure 3a. We choose R_L as a large number (e.g., 100Ω) to also keep efficiency large. Then coils with nine turns would be a good coil size satisfying the aforementioned design specifications. When a marker is placed on a point where R_S and R_L are 50Ω and 100Ω , predicted peak efficiency and critical coupling distances are 0.976 and 23 cm, respectively, as seen in Figure 3d.

4. Measurement results

4.1. Characterization of coils

The coils are fabricated by winding nine circular turns with a radius of 25 cm as designed in the previous section. Coils are characterized first by measuring one port S-parameter (S_{11}) of each coil from 100 KHz to 5 MHz using a Rohde & Schwarz FSH8 Spectrum + Network analyzer. The self-inductance, $L_{1,2}$, of each coil is extracted by resonating out the measured coil with a known capacitor, C , in an RF simulator. From the simulated input impedance (Z_{in_c}) of this resonant coil, one can find the resonance frequency, f_0 , and extract $L_{1,2}$ as follows:

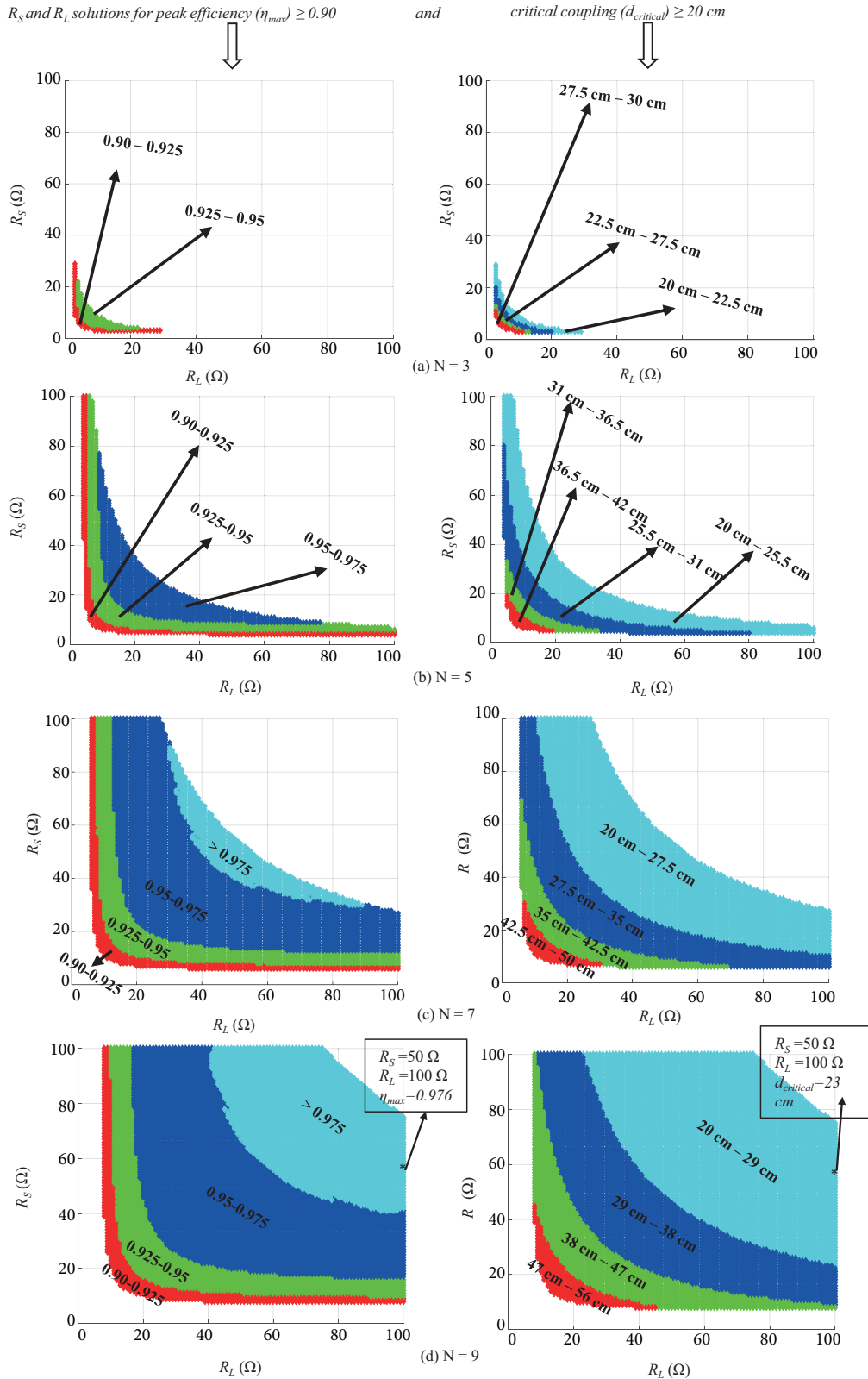


Figure 3. Solutions of R_S and R_L satisfying peak efficiencies larger than 0.90 (left side) and critical coupling distances larger than 20 cm (right side) for (a) $N = 3$, (b) $N = 5$, (c) $N = 7$, and (d) $N = 9$.

Table. Theoretical and measured values of self-inductances and series-connected capacitors for fabricated coils.

	Simulation (circuit model)		Simulation (HFSS)		Measurement	
Coil 1	$L_1=121.7$ uH	$C_1=208$ pF	$L_1=127.9$ uH	$C_1=198$ pF	$L_1=115$ uH	$C_1=220$ pF
Coil 2	$L_2=121.7$ uH	$C_2=208$ pF	$L_2=127.9$ uH	$C_2=198$ pF	$L_2=115$ uH	$C_2=220$ pF

$$L_{1,2} = \frac{1}{(2\pi f_0)^2 \times C}. \quad (13)$$

The extracted (from measurements) and theoretical (from circuit model and HFSS simulations) self-inductance values along with required values for series-connected capacitors for 1 MHz resonance are given in the Table. The designed coils are also simulated using an electromagnetic high frequency structure simulator (HFSS) to study the difference in the efficiency between model and measurement results as will be discussed in the following section. The power transfer efficiency of coupled coils, which are resonated out using 220 pF series-connected lossless capacitors, are calculated from measured S-parameters as follows:

$$\eta = |S_{21}|^2. \quad (14)$$

The port 1 and port 2 impedances, which represent R_S and R_L , are 50 Ω and 100 Ω , respectively, as chosen in the previous section. Figures 4a–4i show the measured power transfer efficiency as a function of frequency for various distances between the coils. Simulated efficiency using Eq. (10) is also plotted on the same graphs for comparison. Peak efficiencies are observed at even and odd mode resonance frequencies (f_{odd} and f_{even}) and the peak efficiencies at f_{even} seem to be higher when the coils operate in the strongly coupled regime. From simulation results, we expected that the efficiencies at f_{odd} would be slightly higher or equal to the efficiencies at f_{even} . The opposite observation in measurement results is due to the detuning at the resonance frequency of either one of the coils. f_{odd} and f_{even} get close to each other and finally merge on the isolated resonance frequency of coils at f_0 of 1 MHz as the distance between the coils increases from 4 cm to approximately 24 cm (d_{critical}). Beyond 24 cm, efficiency peaks are still at 1 MHz, but the peak value reduces as the separation further increases.

4.2. Frequency-tuned wireless power transfer system

A frequency-tuned system is partially set up using the fabricated coils characterized in the previous section. The resonance frequency is tracked by finding the minimum reflection coefficient at the transmitter side because reflected power is almost minimized when maximum possible power is transmitted to the receiver coil, as expected. The block diagram of the frequency-tuned system is shown in Figure 5a. An RF signal generator with source impedance of 50 Ω is connected to the input port of a 20 dB bidirectional coupler. The bidirectional coupler exhibits 50 Ω at all its four ports as well. Therefore, R_S in the frequency-tuned system is 50 Ω , as designed in the previous section. An input matching network (IMN) can be used if an R_S value different from 50 Ω is utilized. The coupler's forward (Forw) and reflect (Refl) ports are connected to 50 Ω resistances (Figure 5a). A load resistance (R_L) of 100 Ω is directly connected to the output of the receive coil. The oscilloscope's three channels are used to measure the voltages on 50 Ω resistances at forward reflect ports of the bidirectional coupler and 100 Ω load resistance. This frequency-tuned system is set up in the laboratory as shown in Figure 5b.

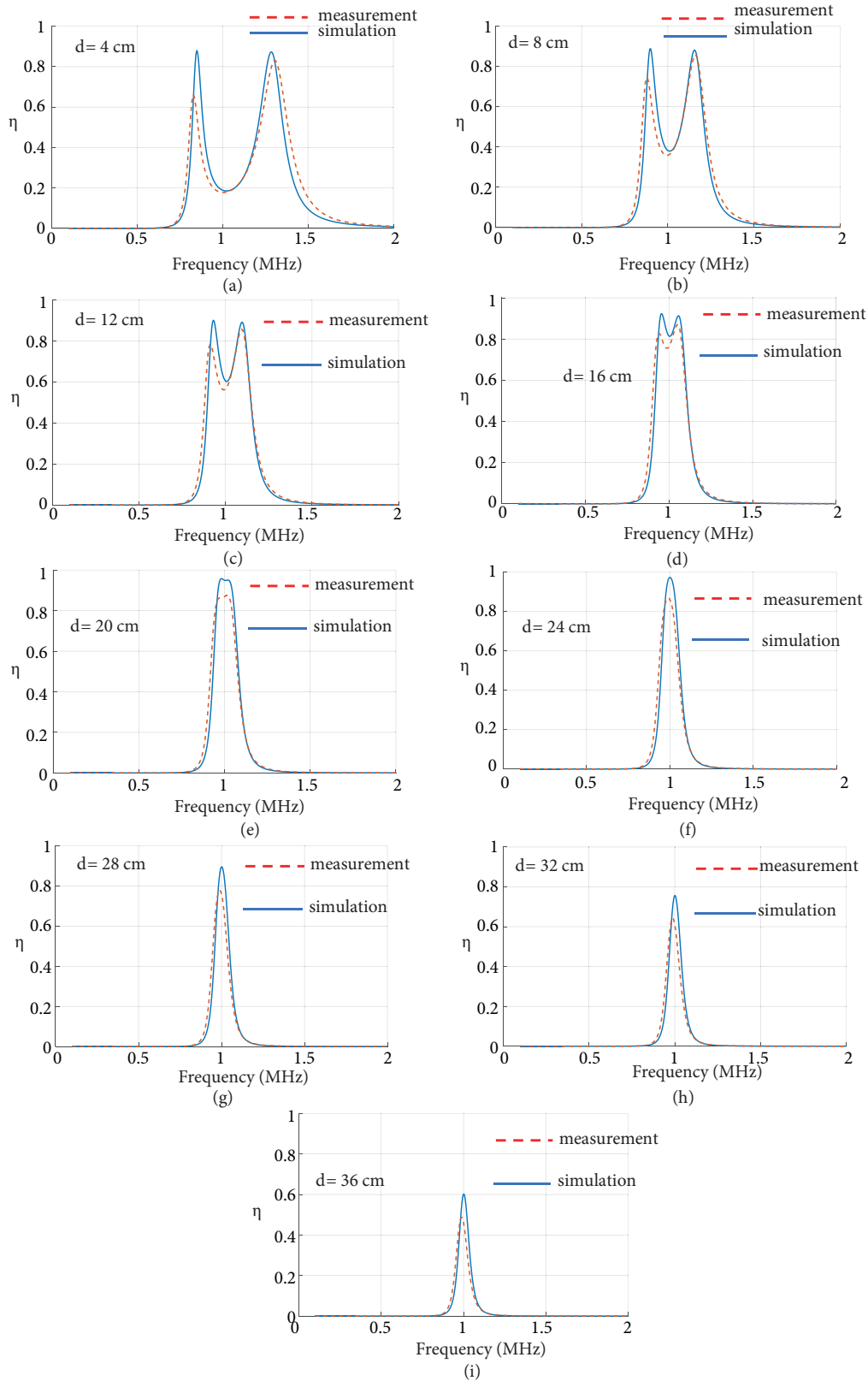


Figure 4. Measured and simulated efficiencies as a function of frequency for coupled resonant coils with separations of (a) 4 cm, (b) 8 cm, (c) 12 cm, (d) 16 cm, (e) 20 cm, (f) 24 cm, (g) 28 cm, (h) 32 cm, and (i) 36 cm.

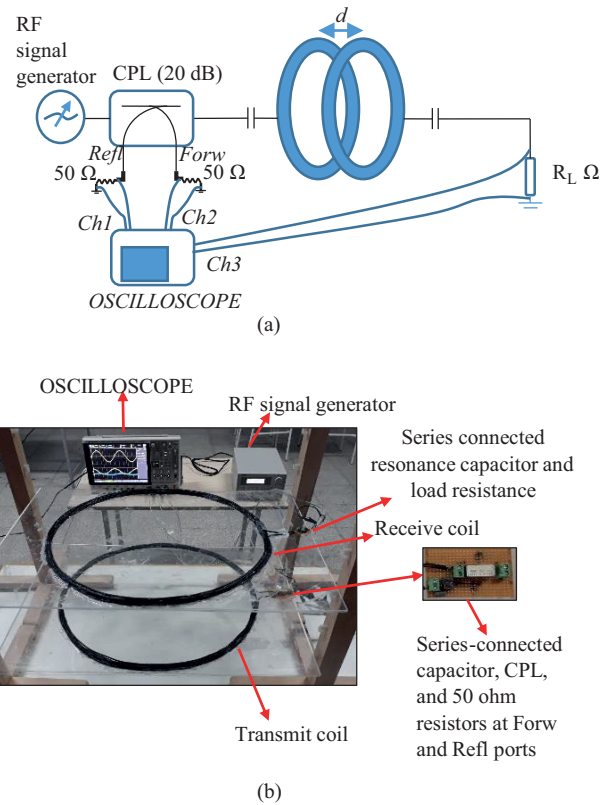


Figure 5. Frequency-tuned system's (a) block diagram and (b) setup's photograph.

The output power of the RF signal generator is set to 7 dBm. The separation between the coils is changed, and at each separation, the frequency of the RF signal generator is varied manually until the power at the reflect port is minimum. This guarantees the frequency of the almost highest power transfer efficiency by just controlling the system at the transmitter side. Figure 6 shows the measured peak efficiency, η_{\max} , at frequencies where the minimum reflection is observed as a function of distance between the coils in the frequency-tuned system. In the same figure, measured peak efficiency using a network analyzer (Figure 4) and simulated peak efficiency using Eq. (10) are also provided for comparison. In frequency-tuned system tests, minimum reflected power levels are observed at f_{even} , which is in accordance with network analyzer measurements. The variations of odd and even mode resonance frequencies are also plotted as a function of distance between the coils and shown in Figure 7.

Measured and simulated resonance frequencies exhibit very good agreement. The peak efficiency varies from 0.77 to 0.80 in the strongly coupled regime up to 24 cm. Such efficiency values are lower than what is predicted from simulated values (Figure 3d).

To better study what causes this difference between circuit model and measurement results, the fabricated coils are simulated in an electromagnetic high frequency structure simulator (HFSS). In the HFSS, first a single (uncoupled) coil is simulated as a 1-port device from 0.5 MHz to 1.5 MHz. The extracted self-inductance and required resonance capacitor values for 1 MHz operation are shown in the Table. Then two identical coupled coils are simulated as a two-port network at loop separations from 4 cm to 36 cm with 4 cm steps. Two port S-parameters from the HFSS simulations are utilized to extract the efficiency of coupled coils by connecting

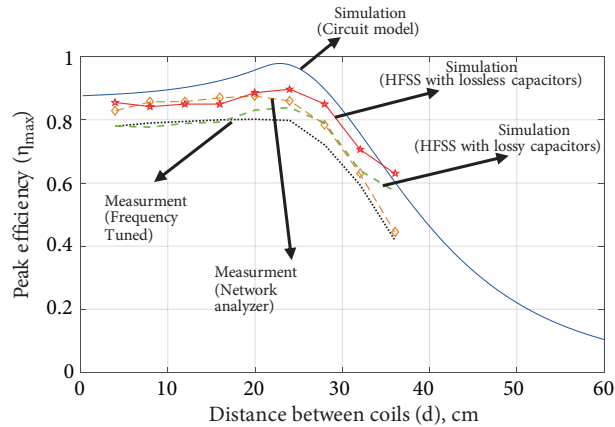


Figure 6. Measured peak efficiency, η_{\max} , at frequencies where minimum reflection is observed, as function distance between the coils in the frequency-tuned system (black dot), measured peak efficiency by network analyzer measurements (brown dashes), and simulated peak efficiencies using circuit model and HFSS.

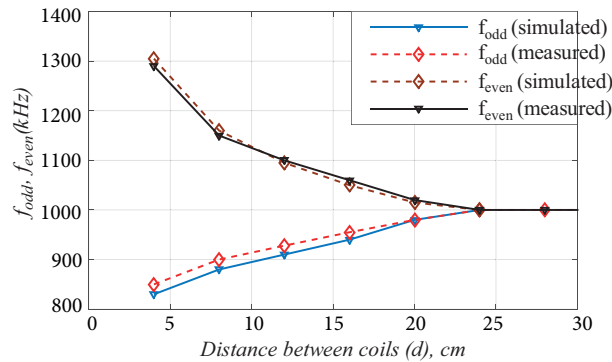


Figure 7. The variation of odd and even mode resonance frequencies as a function of distance between the coils.

resonance capacitors in microwave simulation software. Extracted efficiencies from HFSS simulations as a function of distance are also plotted in Figure 6 for both lossless and lossy resonance capacitors. When series-connected resonance capacitors are lossless, as in the circuit model and network analyzer measurements, HFSS simulation results agree better with network analyzer measurements as compared to circuit model results. Therefore, one can conclude that the widely utilized circuit model for the coupled coils may lack some accuracy due to unaccounted losses such as the proximity effect. The accuracy of the circuit model is expected to be better for lower numbers of turns. When lossy capacitors with Q of 320 at 1 MHz are utilized, HFSS simulation results agree well with the efficiency measurements from the frequency-tuned system.

4.3. Conclusion

We have presented a frequency-tuned wireless power transfer system with near constant efficiency of more than 75% for up to 24 cm coil separations. Sizes of coils were systematically determined for the given design specifications. This work was performed for circular coils considering the possible selection of number of turns and source and load resistances; however, the same design procedure can be applied to any coil shape and carried out to optimize more parameters (such as resonance frequency, radius of the wire, different numbers of turns, and radii of the coils). An important direction of this work is to incorporate various other loss mechanisms, such as proximity losses, into the circuit model to improve the accuracy of model predictions.

Acknowledgment

This research was supported by the Scientific and Technological Research Council of Turkey (Project Number: TÜBİTAK-EEEAG-115E001).

References

- [1] Kurs, A, Karalis, A. Wireless power transfer via strongly coupled magnetic resonances. *Science* 2007; 317: 83-86.
- [2] Karalis A, Joannopoulos JD, Soljacic M. Efficient wireless non-radiative mid-range energy transfer. *Ann Phys-New York* 2008; 323: 34-48.
- [3] Low ZN, Chinga RA, Tseng R, Lin J. Design and test of a high-power high-efficiency loosely coupled planar wireless power transfer system. *IEEE T Ind Electron* 2009; 56: 1801-1812.
- [4] Lim Y, Tang H, Lim S, Park J. An adaptive impedance-matching network based on a novel capacitor matrix for wireless power transfer. *IEEE T Power Electr* 2014; 29: 4403-4413.
- [5] Beh TC, Kato M, Imura T, Oh S, Hori Y. Automated impedance matching system for robust wireless power transfer via magnetic resonance coupling. *IEEE T Ind Electron* 2013; 60: 3689-3698.
- [6] Waters BH, Sample AP, Smith JR. Adaptive impedance matching for magnetically coupled resonators. In: *Progress In Electromagnetics Research Symposium Proceedings*; 19–23 August 2012; Moscow, Russia. pp. 694–701.
- [7] Heibl JD, Thomas EM, Penno RP, Grbic A. Comprehensive analysis and measurement of frequency-tuned and impedance-tuned wireless non-radiative power-transfer systems. *IEEE Antenn Propag M* 2014; 56: 131-148.
- [8] Chen CJ, Chu TH, Lin CL, Jou ZC. A study of loosely coupled coils for wireless power transfer. *IEEE T Circuits-II* 2010; 57: 536-540.
- [9] Budhia M, Covic G, Boys J. A new IPT magnetic coupler for electric vehicle charging systems. In: *IECON 36th Annual Conference on IEEE Industrial Electronics Society*; 7–10 November 2010; Glendale, AZ, USA. New York, NY, USA: IEEE. pp. 2487–2492.
- [10] Covic GA, Kissin ML, Kacprzak D, Clausen N, Hao H. A bipolar primary pad topology for ev stationary charging and highway power by inductive coupling. In: *Energy Conversion Congress and Exposition*; 17–22 September 2011; Phoenix, AZ, USA. New York, NY, USA: IEEE. pp. 1832-1838.
- [11] Villa JL, Sallan J, Osorio JFS, Llombart A. High-misalignment tolerant compensation topology for ICPT systems. *IEEE T Ind Electron* 2012; 59: 945-951.
- [12] Gao Y, Zhou C, Zhou J, Huang X, Yu D. Automatic frequency tuning with power-level tracking system for wireless charging of electric vehicles. In: *Vehicle Power and Propulsion Conference*; 17–20 October 2016; Hangzhou, China. New York, NY, USA: IEEE. pp. 1-5.
- [13] Kar D, Nayak P, Bhuyan S, Panda S. Automatic frequency tuning wireless charging system for enhancement of efficiency. *Electron Lett* 2014; 50: 1868-1870.
- [14] Sis SA, Bıçakcı S. A resonance frequency tracker and source frequency tuner for inductively coupled wireless power transfer systems. In: *46th European Microwave Conference*; 4–6 October 2016; London, UK. New York, NY, USA: IEEE. pp.751-754.
- [15] Luo Y, Yang Y, Chen S, Wen X. A frequency-tracking and impedance-matching combined system for robust wireless power transfer. *Int J Antenn Propag* 2017; 2017: 5719835.
- [16] Sample AP, Smith JR. *Wireless Power Transfer Apparatus and Method Thereof* (2012). US Patent 8,299,652.
- [17] Seo DW, Lee JH. Frequency-tuning method using the reflection coefficient in a wireless power transfer system. *IEEE Microw Wirel Co* 2017; 27: 959-961.
- [18] Bıçakcı S, Sis SA. Rf uygulamalarda genel amaçlı tınlama frekansı takip edici sistem tasarımı. *Gazi University Journal of Science* 2017; 5: 211-221 (in Turkish).

- [19] Ozdemir C, Mete AN. A frequency-tracking algorithm for inductively coupled wireless power transfer systems. In: 10th International Conference on Electrical and Electronics Engineering; November 2017; Bursa, Turkey. pp. 1461-1465.
- [20] Kim N, Kim K, Choi J, Kim CW. Adaptive frequency with power-level tracking system for efficient magnetic resonance wireless power transfer. *Electron Lett* 2012; 48: 452-454.
- [21] Sample AP, Meyer DT, Smith JR. Analysis, experimental results, and range adaptation of magnetically coupled resonators for wireless power transfer. *IEEE T Ind Electron* 2011; 58: 544-554.
- [22] Imura T, Hori Y. Maximizing air gap and efficiency of magnetic resonant coupling for wireless power transfer using equivalent circuit and Neumann formula. *IEEE T Ind Electron* 2011; 58: 4746-4752.
- [23] Imura T, Okabe H, Hori Y. Basic experimental study on helical antennas of wireless power transfer for electric vehicles by using magnetic resonant couplings. In: *Vehicle Power and Propulsion Conference*; 7–10 September 2009; Dearborn, MI, USA. New York, NY, USA: IEEE. pp. 936-940.
- [24] Thomas EM, Heubl JD, Pfeiffer C, Grbic A. A power link study of wireless non-radiative power transfer systems using resonant shielded loops. *IEEE T Circuits-I* 2012; 59: 2125-2136.